https://doi.org/10.5194/egusphere-2024-3046
Preprint. Discussion started: 6 November 2024

New insights into the nonlinear effects of NO_x on SOA formation from isoprene photo-oxidation

Xinbei Xu[1], Yining Gao[1], Si Zhang[1]*, Luyao Chen[1], Rongjie Li[1], Zheng Li[1], Rui Li[1,2], Gehui Wang[1,2]*

[1]Key Laboratory of Geographic Information Science of the Ministry of Education, School of Geographic Sciences, East China Normal University, Shanghai 200241, China
[2]Institute of Eco-Chongming, Cuiniao Road, Chenjia Zhen, Chongming, Shanghai 202150, China

*Correspondence to: Dr. Si Zhang, E-mail address: szhang@geo.ecnu.edu.cn
Prof. Gehui Wang, E-mail address: ghwang@geo.ecnu.edu.cn

https://doi.org/10.5194/egusphere-2024-3046
Preprint. Discussion started: 6 November 2024

Abstract: Atmospheric isoprene can be oxidizene SOA yield on NO_x concentrations was investigated by performing a series of batch chamber experiments; both the gas and aerosol phase chemical species were characterized using High-Resolution Time-of-Flight Chemical Ionization Mass Spectrometer (HR-TOF-CIMS) and High-Resolution Time-of-Flight Aerosol Mass Spectrometer (HR-TOF-AMS), along with an Observation-Based Model (OBM) incorporated with the Master Chemical Mechanism (OBM-MCM model) simulation. We found that NO_x could influence the formation of the ultralow volatility organic compounds(ULVOCs, $\log_{10} C^* < -8.5$), low volatility organic compounds (LVOCs, $-4.5 < \log_{10} C^* < -0.5$) and extremely low volatility organic compounds (ELVOCs, $-8.5 < \log_{10} C^* < -4.5$) by changing the RO_2 fate, which are the critical compounds in nucleation and condensation in particle phase respectively. The SOA of isoprene photooxidation was mainly from RO_2+HO_2 and RO_2+NO pathways. When RO_2+HO_2 was the dominant RO_2 fate, the SOA yield increased with the fraction of RO_2+HO_2 and RO_2+NO increasing. While when NO is the major sink for RO_2, RO_2+NO would inhibit the formation low volatile VOCs and affect the SOA yield. The branching ratio term (β) is used to denote the competitive relationship between the two RO_2 fates (RO_2+HO_2 and RO_2+NO). The loss rate of RO_2+HO_2 pathway was maximized at a branching ratio β of 0.5 ($[NO_x]/[Isoprene]=0.77$), when more low volatiles were produced and the SOA yield reached maximum. The branching rate term (β) can be used as a reference for field campaign and modeling.

Key words: Isoprene; NO_x dependence; SOA yield; HOMs; RO_2 fate.

https://doi.org/10.5194/egusphere-2024-3046
Preprint. Discussion started: 6 November 2024

1. Introduction

Secondary organic aerosol (SOA) is largely formed from photochemical oxidation of anthropogenic and biogenic volatile organic compounds (VOCs), which is a major component of tropospheric fine particles and significantly affect air quality, human health, and climate change (Zhang et al., 2015; Wang et al., 2014; Fan et al., 2008; Pope Iii et al., 2002). With an annual global emission of around 500 Tg yr^{-1}, isoprene is the most prevalent non-methane hydrocarbon (NMHC) released into the atmosphere (Guenther et al., 2006). As a five-carbon conjugated diene, isoprene reacts rapidly with OH and NO_3 radicals and O_3 in the atmosphere to form SOA (Wennberg et al., 2018; Kamens et al., 1982; T. A. Biesenthal, 1998; Nguyen et al., 2010).

NO_x plays an important role in the photooxidation of isoprene in the atmosphere. NO_x can alter the sinks of peroxy radicals (RO_2) produced from the oxidation of isoprene by oxidants and addition of O_2, thus affecting the composition of reaction products such as oligomers and organic nitrates in nucleation and particles growth processes (Surratt et al., 2006). By affecting the branching ratios of the main RO_2 reactions (RO_2+HO_2 and RO_2+NO), NO_x determines the reaction products and final SOA generation of isoprene photooxidation. The RO_2+HO_2 pathway produces organic hydroperoxide species, which is of lower volatility. In contrast, the RO_2+NO pathway generates RO radicals that are fragmented into more volatile products, with a small portion of RO_2 reacting with NO_2 to form relatively lower volatile organic nitrates (Kroll et al., 2006; Wennberg et al., 2018). Changes on NO_x levels can influence the formation of the main oxidants OH, O_3 and NO_3 and thus affect the oxidation process of isoprene (Mayhew et al., 2023). Up to now, researches on isoprene photochemical reaction in the presence of NO_x have focused on the gas- and particle-phase products and chemical mechanism, but few studies have simultaneously and quantitatively investigated the nonlinear effects of NO_x on the isoprene-SOA yield and the fate of RO_2 radicals (Kroll et al., 2005, 2006; Xu et al., 2014; D'ambro et al., 2017; Surratt et al., 2006).

Kroll et al. (2006) and Xu et al. (2014) explored the nonlinear effect of NO_x level on isoprene-SOA mass yield, finding that the SOA yield increased first and then decreased with an increasing NO_x levels. Kroll et al. (2006) reported that the high concentration NO

https://doi.org/10.5194/egusphere-2024-3046
Preprint. Discussion started: 6 November 2024

could suppress the formation of SOA by inhibiting hydroperoxide formation and the SOA is mainly from the oxidation of methacrolein formed from the reaction of RO radicals under high-NO_x conditions. Xu et al. (2014) found that the hydroxyhydroperoxides and dihydroxyepoxides oxidation was the most important pathway of isoprene-SOA formation at low NO_x concentrations, and an increasing NO level could promote the SOA formation by enhancing methacrolein reaction pathway. Besides RO_2 chemistry, the nonlinear influence of NO_x on SOA yield can also be affected by the changes of oxidant concentrations. In the above studies, the additional addition of OH precursors into the reaction system made the OH become the dominant oxidant throughout the reaction due to the continual formation of OH from its precursor photolysis, yet the roles of O_3 and NO_3 were ignored (Kroll et al., 2006; Xu et al., 2014). However, isoprene tends to be synergistically oxidized by multiple oxidants in the real atmosphere (Geyer et al., 2003; Mondal et al., 2021). The ignorance of the synergistic oxidation may bring deviations to the understanding of the photooxidation process of isoprene in the atmosphere especially in urban regions.

In this study, we systematically investigated the SOA formation by photo-oxidation of isoprene in different [NO_x]/[Isoprene] environments, and identified the key factors affecting the SOA yield by analyzing the competition effects between various oxidation pathways. We first explored the direct effect of NO_x on the physical properties of isoprene SOA, then investigated the mechanisms of NO_x on the formation of SOA precursors, finally recognized the changes in RO_2 fate under different NO_x levels conditions.

2 Experiment Section

2.1 Chamber experiments and online monitoring

A home-made 5 m^3 Teflon PFA environmental chamber was used in this study, which is equipped with 365 nm black light bulbs (40 W, F40BLB, GE, USA)(Liu et al., 2021). The chamber was cleaned with dry zero air for at least 12 h prior to each experiment. During the experiments, about 1 ppm of isoprene and different levels NO_x were added into the chamber before the lights were turned on. The detailed experimental conditions were listed in Table 1. All experiments were carried out under dry (<15% RH) conditions. Concentration and size distribution of particles in the chamber throughout the experiments

https://doi.org/10.5194/egusphere-2024-3046
Preprint. Discussion started: 6 November 2024

were detected utilizing a scanning mobility particle sizer (SMPS, 3082, TSI, USA). Chemical composition of aerosols in the chamber was monitored by an online High-Resolution Time-of-Flight Aerosol Mass Spectrometer (HR-ToF-AMS, Aerodyne Research Inc., USA). The variations in the concentrations of isoprene and gas-phase organic products were monitored using a proton transfer reaction Time-of-Flight Mass Spectrometry (PTR-TOF-MS, Ionicon Analytik, Innsbruck, Austria). Nitrogen oxides and ozone were monitored using a NO-NO_2-NO_x analyzer (model 42i, Thermo scientific, USA) and a O_3 analyzer (model 49i, Thermo scientific, USA), respectively. The gas-phase low volatile organic compounds in the chamber were also measured by using nitrate ion time of flight chemical ionization mass spectrometer (NO_3^--ToF-CIMS).

2.2 Wall loss correction and SOA yield calculation

Wall loss has been confirmed to be one of the major factors affecting the accuracy of determining the SOA yield (Zhang et al., 2014). The aerosol mass concentrations were corrected according to Pathak et al. (2007) and Zhang et al. (2024). As the gas-phase VOC wall loss coefficients we calculated was very low, the gas-phase wall losses were neglected in this study. The calculation method for vapor wall loss corrections is detailed in Section S1. Calculating the SOA yield according to the following formula:

$$Y = \frac{\Delta M_0}{\Delta HC} \quad (1)$$

where Y is the SOA yield, ΔM_0 is the maximum concentration of organic aerosols in the chamber (μg m^{-3}), and ΔHC is the concentration of reacted isoprene (μg m^{-3}).

2.3 OBM-MCM model

We use an observation-based model (OBM) incorporated with the Master Chemical Mechanism (MCM) to further investigate the changes in the levels of OH, HO_2 and loss rates of main RO_2 radicals in isoprene photo-oxidation under different NO_x conditions. In this work, the RO_2 self- and cross- reaction chemistry (Wennberg et al., 2018) were added into the latest version 3.3.1 of MCM (MCM v3.3.1; available at https://mcm.york.ac.uk/MCM) to improve the simulation.

3. Results and Discussion

3.1 NO_x dependence on isoprene SOA

https://doi.org/10.5194/egusphere-2024-3046
Preprint. Discussion started: 6 November 2024

Figure 1 shows the time series of NO_x, isoprene, the oxidants O_3 and OH radicals, the main gas organic products methacrolein + methyl vinyl ketone (MACR+MVK, C_4H_6O), and SOA mass concentration in the whole reaction process under 936 ppb isoprene and 712 ppb NO_x condition (Table 1). During the experiment, concentrations of O_3 and OH radicals increased rapidly after the black lights were turned on, which were produced form the reactions of O_2 and H_2O with the oxygen atom formed from the photolysis of NO_2, respectively (Eq. (1-5)) (Seinfeld and Pandis, 2006). Rapid increases in MACR and MVK levels were observed as isoprene was oxidized, which are the first generation of oxidation products in the oxidation process of isoprene by OH radicals and O_3 (Kroll et al., 2006; Nguyen et al., 2016; Galloway et al., 2011). Meantime, a series of complex RO_2 chemistry occurred and produced abundant low volatile organic compounds, such as organic hydroperoxides, organic nitrate and highly oxygenated organic molecules (HOMs) formed from the RO_2+HO_2, RO_2+NO and RO_2 autoxidation, respectively, which undergo nucleation and condensation on particles to generate SOA (Jiang et al., 2017). In the chamber, 80 μg m^{-3} SOA was formed (Figure 1) and the corrected SOA yield was 3.0% (Table 1) under 712 ppb NO_x condition.

$$NO_2+hv \rightarrow NO+O(^3P) \quad (1)$$

$$O(^3P)+O_2 \rightarrow O_3 \quad (2)$$

$$O_3+hv \rightarrow O(^1D)+O_2 \quad (3)$$

$$O(^1D)+H_2O \rightarrow 2OH \quad (4)$$

$$O(^1D) \rightarrow O(^3P) \quad (5)$$

The effect of NO_x on SOA yield was explored and the results are shown in Table 1 and Figure 2a. Obviously, SOA yield showed a trend of first increasing and then decreasing along with an increasing NO_x level, which is consistent with the results reported by Kroll et al. (2006) and Xu et al. (2014). The turning point of SOA yield was at 712 ppb NO_x. Such a dependence of SOA yield on the NO_x levels likely resulted from the difference of gas-phase peroxy radicals (RO_2) chemistry and succeeding particle-phase oligomerization reactions under different NO_x conditions (Xu et al., 2014). Such a SOA yield turning point can also be reflected by the changes of physical properties of the particles in the chamber, such as particle surface area, diameter and number concentration. As shown in Figure 2b and c, both

https://doi.org/10.5194/egusphere-2024-3046
Preprint. Discussion started: 6 November 2024

the number concentrations and particle size increased along with an increasing NO_x level. However, when the NO_x further increased to a level lager than 712 ppb, both started to quickly decrease. The particle diameter and number concentration at 712 ppb NO_x were 1.5 and 1.3 times larger than those at 1500 ppb NO_x, respectively (Figure 2b), indicating an enhanced new particle formation and subsequent particle growth at 712 ppb NO_x level due to much more low volatile products formed. Meanwhile, the bigger particle surface area at 712 ppb NO_x was more favorable for the growth of SOA by condensation than at 1500 ppb NO_x condition. As shown in Figure 2c, the SOA formed under higher NO_x level conditions showed higher OSc. The results were consistent with Li et al. (2022) and Xu et al. (2014), whom found that the O:C ratio increased as [NO_x]/[VOC] increased. OSc of SOA hinges on the SOA composition, which can be attributed to more highly oxygenated products produced from RO_2 chemistry in the gas phase. These results indicate that the SOA formation pathway may be different under the various NO_x levels in the chamber.

3.2 The effects of NO_x levels on SOA precursors

Low-volatile organic products formed from the gas-phase multiple autoxidation and/or bimolecular reactions of RO_2 have been verified to be the pivotal SOA precursors both in nucleation itself and particle growth (Li et al., 2024; Nie et al., 2023). To explore the effect of RO_2 fate on the isoprene-SOA, low volatile organic products in the chamber under different NO_x levels were analyzed by ToF-CIMS equipped with a nitrate ion source. Figure 3 shows the mass spectra of the gas products in the chamber under 712 ppb and 2060 ppb NO_x levels. The product signal intensity was normalized by the sum of ion source signals ($I_{NO3^-}+I_{HNO3NO3^-}+I_{HNO3HNO3NO3^-}$). As shown in Figure 3, monomers $C_5H_{8\text{-}11}N_{2,3}O_{8\text{-}11}$, dimers including $C_6H_{10}N_2O_{14}$, $C_{10}H_{17}N_3O_{14,16}$, and larger oligomers including $C_{12}H_{20}NO_{17}$, $C_{15}H_{20}N_2O_{14}$ and $C_{15}H_{17}N_2O_{17}$ are the most significant signals at different m/z range observed by the CIMS. These low volatile organic products was mainly produced from different RO_2 chemistry (Zhao et al., 2021; Chen et al., 2022).

Figure S1 illustrates the simplified formation mechanism of four monomers in this system. $C_5H_8N_2O_8$ is formed form the H shift and unimolecular autoxidation of the $C_5H_8NO_5$-RO_2. The primary RO_2 radicals $C_5H_9O_3$ could react with NO to produce $C_5H_9NO_4$, which can react with OH radicals and NO sequentially to form $C_5H_{10}N_2O_8$. $C_5H_9O_3$ could also react

https://doi.org/10.5194/egusphere-2024-3046
Preprint. Discussion started: 6 November 2024

with nitrate radicals, NO or HO_2 radicals sequentially to form $C_5H_9N_3O_{10}$ or $C_5H_{10}N_2O_9$. The polymers mainly produced from the RO_2 multiple bimolecular reactions, in which the HOMs accretion products (HOMs-ACCs) generated by RO_2 self- and cross-reactions have an important influence on the generation of new particles (Kulmala et al., 2013; Berndt et al., 2018).

Figures 4a and b show the time series of these products during the reaction. Because the rate coefficients of OH-oxidation were higher than NO_3-oxidation and unimolecular autoxidation, the formation of $C_5H_{10}N_2O_8$ was faster than other products and displayed higher concentration (Wennberg et al., 2018). When the reaction went on for 30 min, particle formation and diameter growth were observed by SMPS (Figure 4c). At the same time, the signals of lower m/z gaseous products rapidly decreased (Figure 4a), but signals of the higher m/z products increased first and then decreased, indicating that the roles of these compounds on SOA formation were different. The latter may be related to the nucleation and generation of new particles, while the former may contribute to the particle growth by condensing on the new particles. Such a conclusion can be confirmed by the volatility of VOCs that determines their effectiveness on SOA formation. The saturation vapor pressure (C^*) of these VOCs were calculated (calculation method shown in Text S2) and the results were displayed in Table S1. Based on the log C^* values, we found that the HOMs-ACCs are ultralow volatility organic compounds(ULVOCs, $\log_{10} C^* < -8.5$), which are the critical compounds in nucleation, and others are low volatility organic compounds (LVOCs, $-4.5 < \log_{10} C^* < -0.5$) and extremely low volatility organic compounds (ELVOCs, $-8.5 < \log_{10} C^* < -4.5$). As the HOMs-ACCs increased, nucleation occurred and new particles were formed. After isoprene were depleted, the increasing of HOMs-ACCs levels ceased and started to reduce, while LVOCs, ELVOCs started to condense on the surface of the new particles, resulting in the increases in particle diameter. The continuous increase of particle diameters after 90 min was mainly due to the condensation of LVOCs and ELVOCs on particles and collision between particles (Tu and Johnston, 2017).

When 2060 ppb of NO_x was injected into the system, as shown in Figures 3 a and b, the signals of most of products are lower obviously than those at 712 ppb NO_x, especially for HOM-ACCs (Figure 3b). Such a similar inhibition of excess NO_x on HOMs formation was

https://doi.org/10.5194/egusphere-2024-3046
Preprint. Discussion started: 6 November 2024

also observed by Rissanen et al. (2018), who found that the addition of excess NO_2 intercepted the autoxidation of the acylperoxy radicals and inhibited gas-phase highly oxidized dimer products in their cyclohexene ozonolysis experiments. Nie et al. (2023) reported that when the reaction of RO_2 with NO became the main sink for RO_2, HOMs production was inhibited in their experiments. These results indicated that the addition of excess NO_x into the chamber could interfere with the formation of E/ULVOC from isoprene-RO_2 autoxidation/bimolecular reaction, thereby terminating the subsequent reaction pathway.

3.3 Relative changes in oxidation pathway

3.3.1 The influence of oxidants on SOA yield

Figure S2 shows the variations in the concentrations of OH and O_3 under different NO_x levels. By calculating the reaction rate constants of isoprene with OH and O_3 (1.0×10^{-10} and 1.3×10^{-17} cm^3 $molecules^{-1}$ s^{-1}, respectively) (Ziemann and Atkinson, 2012) and their concentrations, we found that the reaction rate of isoprene with O_3 was one order of magnitude lower than its reaction with OH. Thus, the OH radicals were much more important than O_3 in the oxidation of isoprene in this study. The concentrations of OH appeared a nonlinear variation trend with the increasing NO_x, similar to the SOA yield. Increasing NO_x can promote the formation of OH radicals via Eq.(1-5) under 365 nm irradiation conditions. However, as shown in Eq.(6), excessively high NO_x consumes OH can also inhibit OH regeneration (Sarrafzadeh et al., 2016). Thus, the variation of OH may be one important reason resulting in the nonlinear effects of NO_x levels on SOA yield .

$$NO_2+OH\rightarrow HNO_3 \quad (6)$$

Generally, the role of NO_3 radicals on SOA formation is ignored, because NO_3 can be photolyzed under irradiation (Stark et al., 2007). However, as mentioned in section 3.2, NO_3 radicals formed from the reaction of NO_x and O_3 could also contribute to the production of HOMs and SOA due to high concentration NO_2 in this study. Hence the role of NO_3 in SOA formation under different NO_x levels was analyzed in this work. Figure S3 shows the NO_3 concentrations during different NO_x levels, which reached up to 0.46 ppb (1.13×10^{10} molecules cm^{-3}), rendering the reaction rates of isoprene with NO_3 similar to that with OH radicals and further suggesting the importance of NO_3 in the oxidation of isoprene. The NO_3 formation was enhanced by the increasing NO_x. However, it was

https://doi.org/10.5194/egusphere-2024-3046
Preprint. Discussion started: 6 November 2024

suppressed by the decreasing NO_3 under very high NO_x concentrations due to the decrease of O_3 levels. Figure S3b shows that the NO_3 concentrations and SOA yield were strongly linearly positively correlated, indicating that the effective contribution of NO_3 on SOA formation.

3.3.2 The influence of RO_2 fate on SOA yield

Different RO_2 fate could be another reason lead to the nonlinear dependence of SOA yield on NO_x levels. To further investigate the difference of RO_2 fate under various NO_x levels, we compute the loss rate of all RO_2 in the complex multigenerational oxidation of isoprene by OH, O_3 and NO_3 at different NO_x levels using OBM-MCM, and then group their reactions into RO_2+NO, RO_2+HO_2 and RO_2+RO_2 (Figure 5a). The concentrations of NO and HO_2 were shown in Figure 5(b). In the presence of NO_x, RO_2+NO and RO_2+HO_2 are the main reactions of RO_2. When the concentration of NO_x < 577 ppb, RO_2+HO_2 was the main RO_2 fate. The concentrations of HO_2 and NO increased along with the increase of NO_x concentrations, leading to an increase in the proportion of RO_2+HO_2 and RO_2+NO. The low volatility hydroperoxides were the main products of RO_2 +HO_2, which can contribute to new particle and SOA formation (Sarrafzadeh et al., 2016; Wennberg et al., 2018; Wang et al., 2023). In addition, when RO_2+NO is not a major sink for RO_2, the enhancement of RO_2+NO could promote the autoxidation of p-HOMs-RO_2 (n_o<7) that can undergo autoxidation to produce HOMs by reacting with non-HOMs-RO_2 that cannot autoxidize (Li et al., 2022). HOMs are low volatility and can condense on particle phase to form SOA. Therefore, the SOA yield increased with the increasing NO_x concentrations. The more HOMs formed, the higher oxidation state of SOA. However, when NO_x > 577 ppb, the concentrations of HO_2 decreased due to being consumed by abundant NO, which caused the decreases of the fraction of RO_2 + HO_2 and the hydroperoxides concentrations. On the contrary, with the elevation of NO, the fraction of RO_2+NO increased. When NO was a major sink for p-HOMs-RO_2, the reaction can generate RO radicals and volatile products but inhibit the autoxidation reaction of p-HOMs-RO_2. Previous studies reported that RO autoxidation also was also an important pathway in HOMs formation (Nie et al., 2023). Therefore, the effect of NO on HOMs formation was nonlinear and complicated. While the influence of NO_2 on HOMs formation was specific, which can abort the chain

https://doi.org/10.5194/egusphere-2024-3046
Preprint. Discussion started: 6 November 2024

reaction of acyl RO_2 (Rissanen, 2018).

The yield turning point for SOA is considered to be the result of competition between the NO and HO_2 reaction pathways, which can be represented by the branching ratio term (β) to denote the competitive relationship between the two RO_2 fates. The β parameter can be calculated using Eq.(7)

$$\beta = \frac{k_{RO_2+NO}[NO]}{k_{RO_2+HO_2}[HO_2]+k_{RO_2+NO}[NO]} \quad (7)$$

where k_{RO_2+NO} (8.8×10^{-12} cm^3 $molec^{-1}$ s^{-1}) and $k_{RO_2+HO_2}$ (17.4×10^{-12} cm^3 $molec^{-1}$ s^{-1}) are the reaction constants of RO_2 with NO and HO_2 (Peng et al., 2022); $[HO_2]$ and [NO] are the gas-phase of concentrations of HO_2 and NO, respectively.

In this study, β presented the same nonlinear dependence with SOA yield (Figure 6). At β of 0.5, the SOA yield was the maximum when the reaction rates of RO_2+HO_2 and RO_2+NO were equal and the $[NO]/[HO_2]$ ratio was 2. It could be assumed that the turning point of SOA yield from isoprene photooxidation may be controlled by $[NO]/[HO_2]$ ratio. The inference was consistent with Kroll et al. (2006). When the $[NO]/[HO_2] < 2$, the RO_2+HO_2 was the dominant fate and the low volatility hydroperoxides were formed; while the RO_2+NO would compete with RO_2+HO_2 and inhibit the formation of the low volatility hydroperoxides when $[NO]/[HO_2] > 2$. Compared with previous work, the $[NO_x]$/[VOCs] ratios corresponding to the yield turning point with or without OH radical precursors in the reaction systems were about 3 and 0.77 (in this work) respectively (Table 2). Higher OH concentration would lead to higher HO_2 and increased the corresponding $[NO_x]$/[Isoprene] ratio of the turning point.

4. Conclusion

In this study, isoprene photo-oxidation experiments with different concentrations of NO_x were carried out and a nonlinear dependence of SOA mass yield on NO_x concentrations was found. In the presence of NO_x, abundant low volatile gaseous organic products can be formed from the gas-phase multiple autoxidation and/or bimolecular reactions of RO_2. ULVOC are the critical compounds in nucleation, and LVOC and ELVOC can condense on the surface of particles readily resulting in increasing in particle diameter. Excess NO_x can

https://doi.org/10.5194/egusphere-2024-3046
Preprint. Discussion started: 6 November 2024

interfere with the formation of E/ULVOC from isoprene-RO_2 autoxidation/bimolecular reaction, thereby suppressed the SOA formation.

The nonlinear dependence of SOA yield is mainly the result of nonlinear variations of oxidants concentrations and competition between RO_2 reaction pathways. Both OH and NO_3 can contribute the SOA formation effectively in the reaction due to the high NO_2 levels. The OBM-MCM model results showed that RO_2+HO_2 and RO_2+NO are the main RO_2 pathways. When RO_2+HO_2 was the dominant RO_2 sink, the enhancement of RO_2+HO_2 and RO_2+NO pathways along with an increasing NO_x level would promote the generation of low volatility gaseous products, thus promoting the generation and growth of new particles. But, with the further increase of NO_x, the RO_2+NO became the main RO_2 pathway, which not only inhibited RO_2 autoxidation reactions, but also inhibited the RO_2+HO_2 pathway, thus affecting nucleation and condensation of low volatility gaseous products. We found that when the proportion of these two pathways is equal, the SOA yield is the highest. These results are important for further understanding of isoprene oxidation in the atmosphere.

Author contributions. GW designed the whole work. XX, SZ and GW performed the data interpretation and wrote the paper. All authors contributed to the paper with useful scientific discussions or comments.

Competing interests. The authors declared that they have no conflict of interest.

Acknowledgements. This work was funded by the National Natural Science Foundation of China (No. U23A2030, 42130704 and 42407137), the National Key Research and Development Program of China (2023YFC3707401).

Reference

Berndt, T., Mentler, B., Scholz, W., Fischer, L., Herrmann, H., Kulmala, M., and Hansel, A.: Accretion Product Formation from Ozonolysis and OH Radical Reaction of alpha-Pinene: Mechanistic Insight and the Influence of Isoprene and Ethylene, Environ. Sci. Technol., 52, 11069-11077, https://doi.org/10.1021/acs.est.8b02210, 2018.

Chan, A. W. H., Chan, M. N., Surratt, J. D., Chhabra, P. S., Loza, C. L., Crounse, J. D., Yee, L. D., Flagan, R. C., Wennberg, P. O., and Seinfeld, J. H.: Role of aldehyde chemistry and NO_x concentrations in secondary organic aerosol formation, Atmos. Chem. and Phys., 10, 7169-7188, https://doi.org/10.5194/acp-10-7169-2010, 2010.

https://doi.org/10.5194/egusphere-2024-3046
Preprint. Discussion started: 6 November 2024

Chen, Y., Tan, Y., Zheng, P., Wang, Z., Zou, Z., Ho, K. F., Lee, S., and Wang, T.: Effect of NO2 on nocturnal chemistry of isoprene: Gaseous oxygenated products and secondary organic aerosol formation, Sci. Total. Environ., 842, 156908, https://doi.org/10.1016/j.scitotenv.2022.156908, 2022.

D'Ambro, E. L., Lee, B. H., Liu, J., Shilling, J. E., Gaston, C. J., Lopez-Hilfiker, F. D., Schobesberger, S., Zaveri, R. A., Mohr, C., Lutz, A., Zhang, Z., Gold, A., Surratt, J. D., Rivera-Rios, J. C., Keutsch, F. N., and Thornton, J. A.: Molecular composition and volatility of isoprene photochemical oxidation secondary organic aerosol under low- and high-NO_x conditions, Atmos. Chem. Phys., 17, 159-174, https://doi.org/10.5194/acp-17-159-2017, 2017.

Fan, J., Zhang, R., Tao, W.-K., and Mohr, K. I.: Effects of aerosol optical properties on deep convective clouds and radiative forcing, J. Geophys. Res.: Atmos., 113, D08209, https://doi.org/10.1029/2007JD009257, 2008.

Galloway, M. M., Huisman, A. J., Yee, L. D., Chan, A. W. H., Loza, C. L., Seinfeld, J. H., and Keutsch, F. N.: Yields of oxidized volatile organic compounds during the OH radical initiated oxidation of isoprene, methyl vinyl ketone, and methacrolein under high-NO_x conditions, Atmos. Chem. Phys., 11, 10779-10790, https://doi.org/10.5194/acp-11-10779-2011, 2011.

Geyer, A., Alicke, B., Ackermann, R., Martinez, M., Harder, H., Brune, W., di Carlo, P., Williams, E., Jobson, T., Hall, S., Shetter, R., and Stutz, J.: Direct observations of daytime NO_3: Implications for urban boundary layer chemistry, J. Geophys. Res.: Atmos., 108(D12), 4368, https://doi.org/10.1029/2002JD002967, 2003.

Guenther, A., Karl, T., Harley, P., Wiedinmyer, C., Palmer, P. I., and Geron, C.: Estimates of global terrestrial isoprene emissions using MEGAN (Model of Emissions of Gases and Aerosols from Nature), Atmos. Chem. Phys., 6, 3181-3210, https://doi.org/10.5194/acp-6-3181-2006, 2006.

Jiang, H., Jang, M., and Yu, Z.: Dithiothreitol activity by particulate oxidizers of SOA produced from photooxidation of hydrocarbons under varied NO_x levels, Atmos. Chem. Phys., 17, 9965-9977, https://doi.org/10.5194/acp-17-9965-2017, 2017.

Kamens, R. M., Gery, M. W., Jeffries, H. E., Jackson, M., and Cole, E. I.: Ozone–isoprene reactions: Product formation and aerosol potential, Int. J. Chem. Kinet., 14, 955-975, https://doi.org/10.1002/kin.550140902, 1982.

Kroll, J. H., Ng, N. L., Murphy, S. M., Flagan, R. C., and Seinfeld, J. H.: Secondary organic aerosol formation from isoprene photooxidation under high-NO_x conditions, Geophys. Res. Lett., 32, L18808, https://doi.org/10.1029/2005gl023637, 2005.

Kroll, J. H., Ng, N. L., Murphy, S. M., Flagan, R. C., and Seinfeld, J. H.: Secondary Organic Aerosol Formation from Isoprene Photooxidation, Environ. Sci. Technol., 40, 1869-1877, https://doi.org/10.1021/es0524301, 2006.

Kulmala, M., Kontkanen, J., Junninen, H., Lehtipalo, K., Manninen, H. E., Nieminen, T., Petäjä, T., Sipilä, M., Schobesberger, S., Rantala, P., Franchin, A., Jokinen, T., Järvinen, E., Äijälä, M., Kangasluoma, J., Hakala, J., Aalto, P. P., Paasonen, P., Mikkilä, J., Vanhanen, J., Aalto, J., Hakola, H., Makkonen, U., Ruuskanen, T., Mauldin, R. L., Duplissy, J., Vehkamäki, H., Bäck, J., Kortelainen, A., Riipinen, I., Kurtén, T., Johnston, M. V., Smith, J. N., Ehn, M., Mentel, T. F., Lehtinen, K. E. J., Laaksonen, A., Kerminen, V.-M., and Worsnop, D. R.: Direct Observations of Atmospheric Aerosol Nucleation, Science, 339, 943-946, https://doi.org/10.1126/science.1227385, 2013.

Li, D., Huang, W., Wang, D., Wang, M., Thornton, J. A., Caudillo, L., Rörup, B., Marten, R., Scholz, W., Finkenzeller, H., Marie, G., Baltensperger, U., Bell, D. M., Brasseur, Z., Curtius, J., Dada, L., Duplissy, J., Gong, X., Hansel, A., He, X.-C., Hofbauer, V., Junninen, H., Krechmer, J. E., Kürten, A., Lamkaddam, H., Lehtipalo, K., Lopez, B., Ma, Y., Mahfouz, N. G. A., Manninen, H. E., Mentler, B., Perrier, S., Petäjä, T., Pfeifer, J., Philippov, M., Schervish, M., Schobesberger, S., Shen, J., Surdu, M., Tomaz, S., Volkamer, R., Wang, X.,

https://doi.org/10.5194/egusphere-2024-3046
Preprint. Discussion started: 6 November 2024

Weber, S. K., Welti, A., Worsnop, D. R., Wu, Y., Yan, C., Zauner-Wieczorek, M., Kulmala, M., Kirkby, J., Donahue, N. M., George, C., El-Haddad, I., Bianchi, F., and Riva, M.: Nitrate Radicals Suppress Biogenic New Particle Formation from Monoterpene Oxidation, Environ. Sci. Technol., https://doi.org/10.1021/acs.est.3c07958, 2024.

Li, Q., Jiang, J., Afreh, I. K., Barsanti, K. C., and Cocker Iii, D. R.: Secondary organic aerosol formation from camphene oxidation: measurements and modeling, Atmos. Chem. Phys., 22, 3131-3147, https://doi.org/10.5194/acp-22-3131-2022, 2022.

Liu, S., Huang, D., Wang, Y., Zhang, S., Liu, X., Wu, C., Du, W., and Wang, G.: Synergetic effects of NH_3 and NO_x on the production and optical absorption of secondary organic aerosol formation from toluene photooxidation, Atmos. Chem. Phys., 21, 17759-17773, https://doi.org/10.5194/acp-21-17759-2021, 2021.

Mayhew, A. W., Edwards, P. M., and Hamilton, J. F.: Daytime isoprene nitrates under changing NO_x and O_3, Atmos. Chem. Phys., 23, 8473-8485, https://doi.org/10.5194/acp-23-8473-2023, 2023.

Mondal, K., Biswas, S., Chattopadhyay, A., Chatterjee, P., and Chakraborty, T.: Gas-Phase Oxidation of NO_2 to HNO_3 by Phenol: Atmospheric Implications, ACS Earth and Space Chemistry, 5, 2131-2141, https://doi.org/10.1021/acsearthspacechem.1c00167, 2021.

Nguyen, T. B., Bateman, A. P., Bones, D. L., Nizkorodov, S. A., Laskin, J., and Laskin, A.: High-resolution mass spectrometry analysis of secondary organic aerosol generated by ozonolysis of isoprene, Atmos. Environ., 44, 1032-1042, https://doi.org/10.1016/j.atmosenv.2009.12.019, 2010.

Nguyen, T. B., Tyndall, G. S., Crounse, J. D., Teng, A. P., Bates, K. H., Schwantes, R. H., Coggon, M. M., Zhang, L., Feiner, P., Millller, D. O., Skog, K. M., Rivera-Rios, J. C., Dorris, M., Olson, K. F., Koss, A., Wild, R. J., Brown, S. S., Goldstein, A. H., de Gouw, J. A., Brune, W. H., Keutsch, F. N., Seinfeld, J. H., and Wennberg, P. O.: Atmospheric fates of Criegee intermediates in the ozonolysis of isoprene, Phys. Chem. Chem. Phys., 18, 10241-10254, https://doi.org/10.1039/c6cp00053c, 2016.

Nie, W., Yan, C., Yang, L., Roldin, P., Liu, Y., Vogel, A. L., Molteni, U., Stolzenburg, D., Finkenzeller, H., Amorim, A., Bianchi, F., Curtius, J., Dada, L., Draper, D. C., Duplissy, J., Hansel, A., He, X. C., Hofbauer, V., Jokinen, T., Kim, C., Lehtipalo, K., Nichman, L., Mauldin, R. L., Makhmutov, V., Mentler, B., Mizelli-Ojdanic, A., Petaja, T., Quelever, L. L. J., Schallhart, S., Simon, M., Tauber, C., Tome, A., Volkamer, R., Wagner, A. C., Wagner, R., Wang, M., Ye, P., Li, H., Huang, W., Qi, X., Lou, S., Liu, T., Chi, X., Dommen, J., Baltensperger, U., El Haddad, I., Kirkby, J., Worsnop, D., Kulmala, M., Donahue, N. M., Ehn, M., and Ding, A.: NO at low concentration can enhance the formation of highly oxygenated biogenic molecules in the atmosphere, Nat. Commun., 14, 3347, https://doi.org/10.1038/s41467-023-39066-4, 2023.

Pathak, R. K., Stanier, C. O., Donahue, N. M., and Pandis, S. N.: Ozonolysis of α-pinene at atmospherically relevant concentrations: Temperature dependence of aerosol mass fractions (yields), J. Geophys. Res.: Atmos., 112, D03201, https://doi.org/10.1029/2006jd007436, 2007.

Peng, W., Le, C., Porter, W. C., and Cocker, D. R., 3rd: Variability in Aromatic Aerosol Yields under Very Low NO_x Conditions at Different HO_2/RO_2 Regimes, Environ. Sci. Technol., 56, 750-760, https://doi.org/10.1021/acs.est.1c04392, 2022.

Pope III, C. A., Burnett, R. T., Thun, M. J., Calle, E. E., Krewski, D., Ito, K., and Thurston, G. D.: Lung Cancer, Cardiopulmonary Mortality, and Long-term Exposure to Fine Particulate Air Pollution, JAMA., 287, 1132-1141, https://doi.org/10.1001/jama.287.9.1132, 2002.

Rissanen, M. P.: NO_2 Suppression of Autoxidation-Inhibition of Gas-Phase Highly Oxidized Dimer Product Formation, ACS Earth Space Chem., 2, 1211-1219, 10.1021/acsearthspacechem.8b00123, 2018.

Sarrafzadeh, M., Wildt, J., Pullinen, I., Springer, M., Kleist, E., Tillmann, R., Schmitt, S. H., Wu, C., Mentel, T. F., Zhao, D., Hastie, D. R., and Kiendler-Scharr, A.: Impact of NO_x and OH on secondary organic aerosol

https://doi.org/10.5194/egusphere-2024-3046
Preprint. Discussion started: 6 November 2024

formation from α-pinene photooxidation, Atmos. Chem. Phys., 16, 11237-11248, https://doi.org/10.5194/acp-16-11237-2016, 2016.

Seinfeld, J. H. and Pandis, S. N.: ATMOSPHERIC CHEMISTRY AND PHYSICS: from air pollution to climate change, John Wliey & Sons 2006.

Stark, H., Lerner, B. M., Schmitt, R., Jakoubek, R., Williams, E. J., Ryerson, T. B., Sueper, D. T., Parrish, D. D., and Fehsenfeld, F. C.: Atmospheric in situ measurement of nitrate radical (NO_3) and other photolysis rates using spectroradiometry and filter radiometry, J. Geophys. Res.: Atmos., 112, D10SO4. https://doi.org/10.1029/2006jd007578, 2007.

Surratt, J. D., Murphy, S. M., Kroll, J. H., Ng, N. L., Hildebrandt, L., Sorooshian, A., Szmigielski, R., Vermeylen, R., Maenhaut, W., Claeys, M., Flagan, R. C., and Seinfeld, J. H.: Chemical Composition of Secondary Organic Aerosol Formed from the Photooxidation of Isoprene, J. Phys. Chem. A, 110, 9665-9690, https://doi.org/10.1021/jp061734m, 2006.

T. A. Biesenthal, J. W. B., P. B. Shepson, S.-M. Li, P. C. Brickell: The chemistry of biogenic hydrocarbons at a rural site in eastern Canada, J. Geophys. Res.: Atmos., 103, 25487-25498, https://doi.org/10.1029/98JD01848, 1998.

Tu, P. and Johnston, M. V.: Particle size dependence of biogenic secondary organic aerosol molecular composition, Atmos. Chem. Phys., 17, 7593-7603, https://doi.org/10.5194/acp-17-7593-2017, 2017.

Wang, S., Zhao, Y., Chan, A. W. H., Yao, M., Chen, Z., and Abbatt, J. P. D.: Organic Peroxides in Aerosol: Key Reactive Intermediates for Multiphase Processes in the Atmosphere, Chem. Rev., 123, 1635-1679, https://doi.org/10.1021/acs.chemrev.2c00430, 2023.

Wang, Y., Wang, M., Zhang, R., Ghan, S. J., Lin, Y., Hu, J., Pan, B., Levy, M., Jiang, J. H., and Molina, M. J.: Assessing the effects of anthropogenic aerosols on Pacific storm track using a multiscale global climate model, Proc. Natl. Acad. Sci. U.S.A., 111, 6894-6899, https://doi.org/10.1073/pnas.1403364111, 2014.

Wennberg, P. O., Bates, K. H., Crounse, J. D., Dodson, L. G., McVay, R. C., Mertens, L. A., Nguyen, T. B., Praske, E., Schwantes, R. H., Smarte, M. D., St Clair, J. M., Teng, A. P., Zhang, X., and Seinfeld, J. H.: Gas-Phase Reactions of Isoprene and Its Major Oxidation Products, Chem. Rev., 118, 3337-3390, https://doi.org/10.1021/acs.chemrev.7b00439, 2018.

Wu, R., Vereecken, L., Tsiligiannis, E., Kang, S., Albrecht, S. R., Hantschke, L., Zhao, D., Novelli, A., Fuchs, H., Tillmann, R., Hohaus, T., Carlsson, P. T. M., Shenolikar, J., Bernard, F., Crowley, J. N., Fry, J. L., Brownwood, B., Thornton, J. A., Brown, S. S., Kiendler-Scharr, A., Wahner, A., Hallquist, M., and Mentel, T. F.: Molecular composition and volatility of multi-generation products formed from isoprene oxidation by nitrate radical, Atmos. Chem. Phys., 21, 10799-10824, https://doi.org/10.5194/acp-21-10799-2021, 2021.

Xu, L., Kollman, M. S., Song, C., Shilling, J. E., and Ng, N. L.: Effects of NO_x on the volatility of secondary organic aerosol from isoprene photooxidation, Environ. Sci. Technol., 48, 2253-2262, https://doi.org/10.1021/es404842g, 2014.

Zhang, R., Wang, G., Guo, S., Zamora, M. L., Ying, Q., Lin, Y., Wang, W., Hu, M., and Wang, Y.: Formation of urban fine particulate matter, Chem. Rev., 115, 3803-3855, https://doi.org/10.1021/acs.chemrev.5b00067, 2015.

Zhang, S., Li, D., Ge, S., Wu, C., Xu, X., Liu, X., Li, R., Zhang, F., and Wang, G.: Elucidating the mechanism on the transition-metal ion-synergetic-catalyzed oxidation of SO_2 with implications for sulfate formation in Beijing haze, Environ. Sci. Technol., 58, 2912-2921, https://doi.org/10.1021/acs.est.3c08411, 2024.

Zhang, X., Cappa, C. D., Jathar, S. H., McVay, R. C., Ensberg, J. J., Kleeman, M. J., and Seinfeld, J. H.: Influence of vapor wall loss in laboratory chambers on yields of secondary organic aerosol, Proc. Natl. Acad. Sci. U.S.A., 111, 5802-5807, https://doi.org/10.1073/pnas.1404727111, 2014.

https://doi.org/10.5194/egusphere-2024-3046
Preprint. Discussion started: 6 November 2024

475 Zhao, D., Pullinen, I., Fuchs, H., Schrade, S., Wu, R., Acir, I.-H., Tillmann, R., Rohrer, F., Wildt, J., Guo, Y.,
476 Kiendler-Scharr, A., Wahner, A., Kang, S., Vereecken, L., and Mentel, T. F.: Highly oxygenated organic
477 molecule (HOM) formation in the isoprene oxidation by NO_3 radical, Atmos. Chem. Phys., 21, 9681-9704,
478 https://doi.org/10.5194/acp-21-9681-2021, 2021.
479 Ziemann, P. J. and Atkinson, R.: Kinetics, products, and mechanisms of secondary organic aerosol formation,
480 Chem. Soc. Rev., 41, 6582-6605, https://doi.org/10.1039/c2cs35122f, 2012.
481
482

https://doi.org/10.5194/egusphere-2024-3046
Preprint. Discussion started: 6 November 2024

Figure Captions

Figure 1. Time profiles for a typical experiment (exp. 5).

Figure 2. NO_x dependence of SOA : (a) SOA yield. (b) Particle surface, diameter and particle number concentration at the highest SOA mass. (c) OS_C from AMS

Figure 3. An example of NO_3^- chemical ionization mass spectra illustrating the suppression of highly oxygenated organic molecules formation by NO_x. The upper panel shows spectrum measured at 712 ppb NO_x (the highest yield level) and the lower panel shows the spectrum measured at 2060 ppb NO_x (excess NO_x, no SOA was produced). Both experiments were measured throughout using ToF-CIMS only. Gas phase species identification is based on the literature references as follows: (a) Chen et al. (2022), (b) Zhao et al. (2021), (c) Rissanen (2018), (d) Wu et al. (2021).

Figure 4. Isoprene SOA nucleation process: (a) evolution of key HOMs detected by ToF-CIMS under 712 ppb NO_x condition; (b) evolution of key HOMs-ACCs detected by ToF-CIMS under 712 ppb NO_x condition; (c) particle diameter detected by SMPS under 712 ppb NO_x condition.

Figure 5. (a)Loss rates of main RO_2 from different oxidation pathways as a function of NO_x concentration calculated by MCMv3.3.1. (b) Variations of NO and HO_2 concentrations.

Figure 6. The relationship between β and SOA yield; color mapping from NO_x.

https://doi.org/10.5194/egusphere-2024-3046
Preprint. Discussion started: 6 November 2024

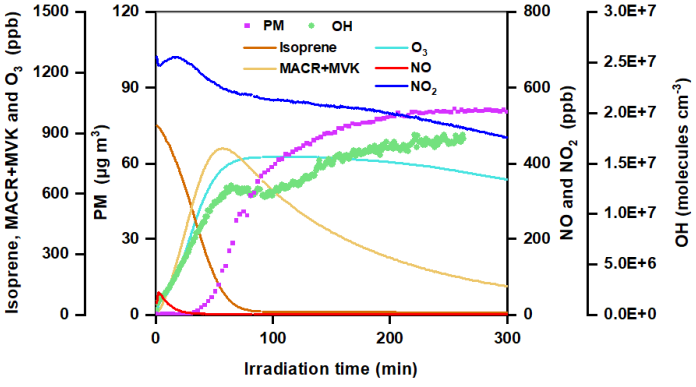

511

512 **Figure 1.** Time profiles for a typical experiment (exp. 5).

513

514

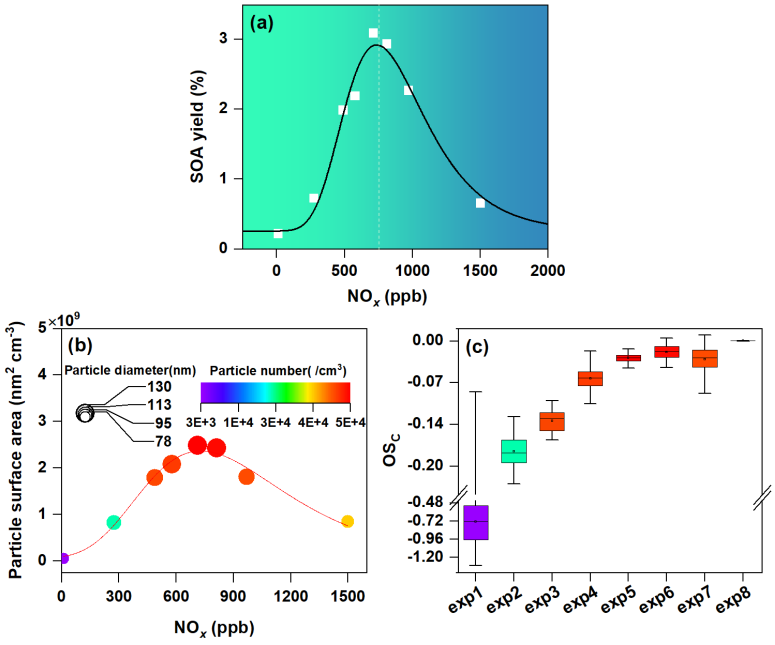

515

516 **Figure 2**. NO_x dependence of SOA : (a) SOA yield. (b) Particle surface, diameter and particle number
517 concentration at the highest SOA mass. (c) OS_C from AMS

518

https://doi.org/10.5194/egusphere-2024-3046
Preprint. Discussion started: 6 November 2024

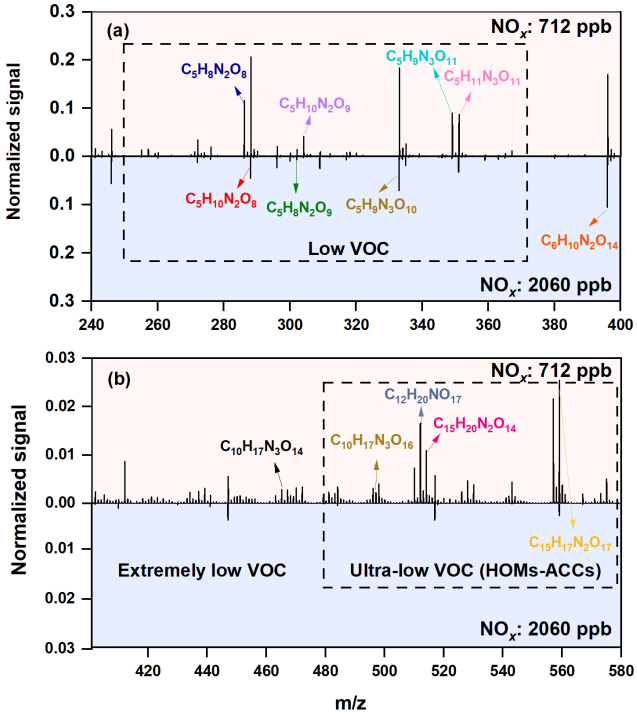

519

520 **Figure 3.** An example of NO_3^- chemical ionization mass spectra illustrating the suppression of highly
521 oxygenated organic molecules formation by NO_x. The upper panel shows spectrum measured at 712 ppb
522 NO_x (the highest yield level) and the lower panel shows the spectrum measured at 2060 ppb NO_x
523 (excess NO_x, no SOA was produced). Both experiments were measured throughout using ToF-CIMS
524 only. Gas phase species identification is based on the literature references as follows: (a) Chen et al.
525 (2022), (b) Zhao et al. (2021), (c)Rissanen (2018), (d) Wu et al. (2021).

526

https://doi.org/10.5194/egusphere-2024-3046
Preprint. Discussion started: 6 November 2024

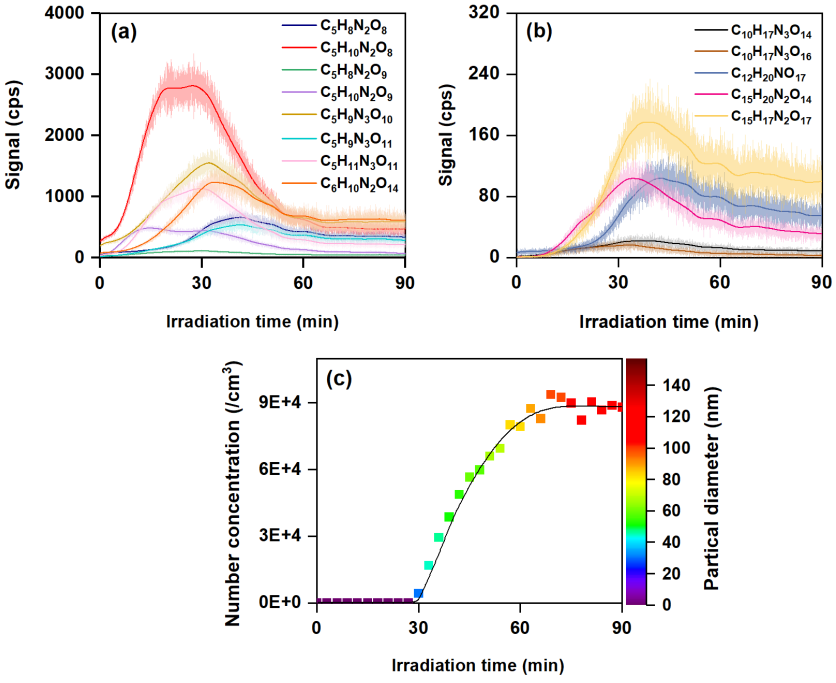

Figure 4. Isoprene SOA nucleation process: (a) evolution of key HOMs detected by ToF-CIMS under 712 ppb NO_x condition; (b) evolution of key HOMs-ACCs detected by ToF-CIMS under 712 ppb NO_x condition; (c) particle diameter detected by SMPS under 712 ppb NO_x condition.

https://doi.org/10.5194/egusphere-2024-3046
Preprint. Discussion started: 6 November 2024

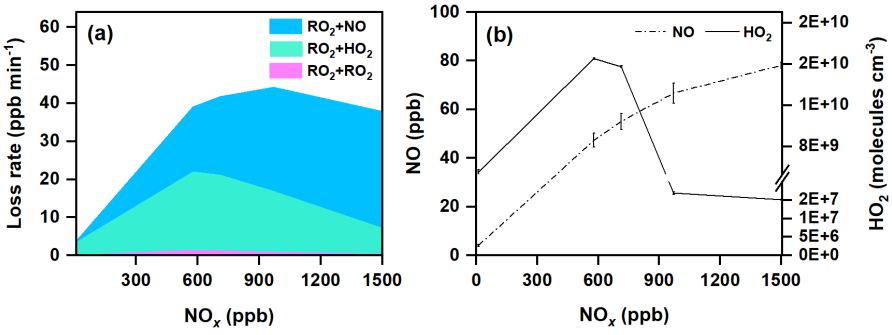

Figure 5. (a)Loss rates of main RO_2 from different oxidation pathways as a function of NO_x concentration calculated by MCMv3.3.1. (b) Variations of NO and HO_2 concentrations.

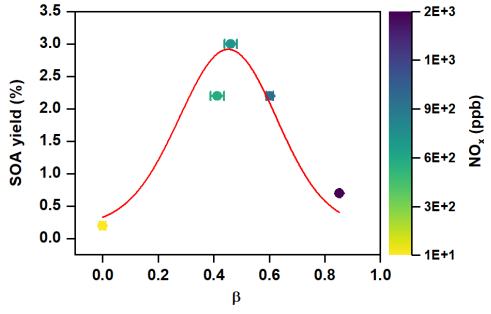

Figure 6. The relationship between β and SOA yield; color mapping from NO_x.

https://doi.org/10.5194/egusphere-2024-3046
Preprint. Discussion started: 6 November 2024

Table Captions

Table 1. Detailed experimental conditions in this Study.

Table 2. The ratio of productivity turning point and corresponding production field in different VOC-OH oxidations experiments.

https://doi.org/10.5194/egusphere-2024-3046
Preprint. Discussion started: 6 November 2024

Table 1. Detailed experimental conditions in this Study.

Exp. no	ISOP (ppb)	NO_0 (ppb)	$NO_{2,0}$ (ppb)	$NO_{x,0}$ (ppb)	$[NO_x]_0/[ISOP]_0$ (ppb ppb^{-1})	**Δ**ISOP (ppb)	O_3 (ppb)	**Δ**M (μg m^{-3})	SOA yield (%)	Corrected SOA yield (%)
1	996	4	6	10	0.01	153	32	1.1	0.1%	0.2%
2	1030	18	255	273	0.27	975	466	20.0	0.6%	0.7%
3	890	7	481	488	0.55	877	734	49.2	1.5%	2.0%
4	989	20	557	577	0.58	976	703	60.3	1.7%	2.2%
5	936	29	683	712	0.76	925	783	80.6	2.3%	3.0%
6	939	40	770	811	0.86	927	818	76.7	2.2%	2.9%
7	957	43	927	970	1.01	948	879	60.7	1.4%	2.2%
8	976	49	1451	1500	1.54	962	708	17.8	0.6%	0.7%
9	1014	60	2000	2060	2.03	985	301	-	-	-

Table 2. The ratio of productivity turning point and corresponding production field in different VOC-OH oxidations experiments.

VOC	Seed	OH precursor	RH (%)	$[NO_x]/[VOC]$	SOA yield (%)	Reference
Isoprene	/	/	<15	0.77	3.0	This study
Isoprene	$(NH4)_2SO_4$	H_2O_2	<10	3.0	5.5	Kroll et al. (2006)
Isoprene	/	H_2O_2	<5	3.0	8.5	Xu et al. (2014)
Isoprene	/	CH_3ONO	9-11	5.0	7.4	Chan et al. (2010)